

Renner–Teller Bending Frequencies of the $\tilde{A} \ ^2\Pi$ State of OCS^+

Steven E. Wheeler, Andrew C. Simmonett, and Henry F. Schaefer, III*

Center for Computational Chemistry, University of Georgia, Athens, Georgia 30602

Received: February 12, 2007; In Final Form: March 12, 2007

There are inconsistencies among previously reported Renner–Teller bending frequencies for the $\tilde{A} \ ^2\Pi$ state of OCS^+ . To resolve these controversies, we have computed vibrational frequencies using high-level excited electronic state ab initio equation-of-motion coupled cluster methods. On the basis of equation-of-motion coupled cluster theory including single, double, and iterative inclusion of partial triple excitations (EOM-CC3) paired with the correlation-consistent polarized valence quadruple- ζ basis set (cc-pVQZ), we predict harmonic bending frequencies of 364 and 401 cm^{-1} for the A' and A'' components of $\tilde{A} \ ^2\Pi \text{OCS}^+$, respectively. Particularly for the upper Renner–Teller component, these results are lower than the theoretical predictions of 370 and 459 cm^{-1} reported by Chen, Hochlaf, Rosmus, He, and Ng [*J. Chem. Phys.* **2002**, *116*, 5612]. Instead, the presently computed bending frequencies are more consistent with the experimentally derived average value of $357 \pm 5 \text{ cm}^{-1}$ recently reported by Sommovilla and Merkt [*J. Phys. Chem. A* **2004**, *108*, 9970], lending credence to the spectral assignments made in this later work. The two components of the Renner–Teller bending frequencies of $\tilde{X} \ ^2\Pi \text{OCS}^+$ are similarly predicted to be 396 and 453 cm^{-1} . Anharmonicity constants arising from a quartic force field computed at the cc-pVQZ EOM-CC3 level of theory are given, to provide a more complete characterization of the potential energy surface of the $\tilde{A} \ ^2\Pi$ state of OCS^+ .

I. Introduction

Linear triatomic molecules offer an ideal target for both extremely high-accuracy theoretical treatments and high-resolution spectroscopic techniques, allowing for the detailed exploration of fundamental physical processes including Fermi resonance, the Renner–Teller effect, and spin–orbit interactions, among others. While there have been numerous spectroscopic studies of the ionized states of OCS ,^{1–23} vanishing Frank–Condon factors have plagued experimental determinations of the Renner–Teller split bending frequencies of the $\tilde{A} \ ^2\Pi$ state of OCS^+ . Indeed, the congested $\tilde{X} \ ^1\Sigma^+ \rightarrow \tilde{A} \ ^2\Pi$ photoionization spectrum of OCS is the least well characterized of the photoionization bands associated with low-lying states of OCS^+ .²³ Nonetheless, experimental estimates^{10,14,19,22} of the bending frequency based on the allowed 2_1^+ hot band have been made, falling in the range of 340–380 cm^{-1} . Other estimates,^{14,19} based on weak spectral features assigned to transitions out of the ground neutral vibronic state were somewhat higher, ranging from 400 to 590 cm^{-1} .

There have also been numerous theoretical studies of the $\tilde{A} \ ^2\Pi$ state of OCS^+ in the past decade.^{20,22,24–28} In 1996, Hubin-Franskin et al.²⁰ presented a joint experimental–theoretical study examining low-lying electronic states of OCS^+ using the TPEPICO method as well as ab initio computed potential energy surfaces for the O–C and C–S stretching coordinates. In 2001, Takeshita, Shida, and Miyoshi examined²⁴ the vibrational structure of photoelectron spectra based on comparisons with simulated ionization intensity curves. Featured in this work were harmonic vibrational frequencies for the O–C and C–S stretching modes for a number of low-lying electronic states computed using multireference configuration interaction, though a treatment of the bending potential was absent.

In 2002, Chen, Hochlaf, Rosmus, He, and Ng²² presented work using multireference configuration interaction computations to help assign the complex PFI-ZEKE photoelectron spectrum associated with the $\tilde{X} \rightarrow \tilde{A}^+$ transition in OCS . Harmonic and anharmonic vibrational frequencies for the $\tilde{A} \ ^2\Pi$ state of OCS^+ were computed by using state-averaged complete active space self-consistent field (SA-CASSCF) and internally contracted multiconfiguration configuration interaction (ic-MRCD), coupled with a truncated cc-pVQZ basis set (in which the g function was stripped from sulfur). Through comparisons with these computed values, many bands in the complex photoelectron spectrum were assigned, at least tentatively. Most notably, the Renner–Teller bending frequencies for the $\tilde{A} \ ^2\Pi$ state of OCS^+ were predicted to be 370 and 459 cm^{-1} for the A' and A'' components, respectively, corresponding to a root-mean-square value of 417 cm^{-1} . Subsequently, a high-accuracy spectroscopic study was published by Sommovilla and Merkt²³ examining the Renner–Teller effect in the $\tilde{A} \ ^2\Pi$ state of OCS^+ , yielding a recommended average bending frequency $\omega_2 = 357 \pm 5 \text{ cm}^{-1}$. In this work, characteristics of the bending energy surface were gleaned from perturbations of the C–S stretching levels caused by Fermi interactions with the bending levels.

While the assignments of the two main features of the PFI-ZEKE spectra are in agreement between the works of Sommovilla and Merkt²³ and Chen et al.,²² assignments of weaker features differed markedly between the two studies. Indeed, the differences are so profound in assignments of the higher Fermi polyads that no common assignments can be found in the two studies. The primary cause for the difference in the two sets of assignments arises from different values for the bending frequency: the value recommended by Sommovilla and Merkt is less than half of the C–S stretching frequency ($809 \pm 6 \text{ cm}^{-1}$) while in the analysis of Chen et al. the bending frequency used is more than half of the C–S stretching

* Corresponding author. E-mail: hfs@uga.edu.

frequency, resulting in drastically different patterns of predicted Fermi interactions.

More recently there have been several purely theoretical forays^{25–28} aimed toward characterizing the potential energy surface of the $\tilde{A}^2\Pi$ state of OCS^+ , though none have focused on the Renner–Teller bending frequencies: Chen, Huang, and Chang examined^{25,26} low-lying electronic states and dissociation channels of OCS^+ using complete active space second-order perturbation theory; Masuda, Hatsui, and Kosugi²⁸ presented excitation energies for low-lying states based on MRCI computations including single, double, and triple excitations; and Hirst computed²⁷ potential energy surfaces for six electronic states using MRCI.

In the present work we seek to dispel lingering uncertainties in the harmonic bending frequencies for the $\tilde{A}^2\Pi$ state of OCS^+ through the use of equation-of-motion coupled cluster methods paired with a quadruple- ζ quality basis set. Yamaguchi and Schaefer found²⁹ fair agreement between experimental results and the predicted Renner–Teller parameter (ϵ) and average harmonic bending frequency for the $\tilde{A}^3\Pi$ state of CNN based on EOM-CCSD computations. By explicitly accounting for the effect of triple excitations in the present work via the EOM-CC3 method, more reliable vibrational frequencies are obtained.

II. Theoretical Methods

The dominant electron configuration for the neutral OCS ground electronic state is written as $[\text{core}](6\sigma)^2(7\sigma)^2(8\sigma)^2(9\sigma)^2(2\pi)^4(3\pi)^4$. The lowest lying ionized states are then dominated by configurations arising from the removal of an electron from the 3π or 2π orbital, giving rise to the $\tilde{X}^2\Pi$ and $\tilde{A}^2\Pi$ states of OCS^+ , respectively. The geometry of the $\tilde{X}^2\Pi$ state of OCS^+ was optimized by using coupled cluster theory with single and double excitations (CCSD),^{30–33} and either partial (CC3)^{34–36} or full inclusion of triple excitations (CCSDT),^{37–40} paired with the correlation consistent polarized valence hierarchy of basis sets,⁴¹ cc-pVXZ ($X = \text{D, T, Q}$ for CCSD and CC3; $X = \text{D, T}$ for CCSDT). The geometry of $\tilde{A}^2\Pi$ OCS^+ was optimized by using excited electronic state ab initio equation-of-motion coupled cluster theory methods⁴² including single and double excitations (EOM-CCSD)^{42,43} and with single, double, and iterative partial triple excitations (EOM-CC3)⁴⁴ paired with the cc-pVXZ ($X = \text{D, T, Q}$) basis sets. The EOM-CC3 method was implemented for open-shell systems for the first time only recently.⁴⁴ Sattelmeyer, Stanton, Olsen, and Gauss examined⁴⁵ the performance of iterative triples linear response coupled cluster methods in the prediction of excited-state properties. The EOM-CC3 approach was shown to offer improvement over EOM-CCSD compared to experimentally derived harmonic vibrational frequencies.

The EOM formalism⁴² allows the straightforward application of the robust coupled cluster theory to excited electronic states. Thus, accurate coupled cluster energies of $\tilde{A}^2\Pi$ OCS^+ can be computed straightforwardly based on Hartree–Fock orbitals from the $\tilde{X}^2\Pi$ state. The reference electronic wave functions were computed by using spin-restricted Hartree–Fock theory (ROHF) to avoid complications arising from a spin-contaminated reference wave function. The ROHF molecular orbitals resembling the $1s$ orbitals on oxygen and carbon and the $1s$, $2s$, and $2p$ orbitals on sulfur were frozen in all correlated computations. The CCSD, CC3, EOM-CCSD, and EOM-CC3 electronic structure computations were carried out with Psi 3.2,⁴⁶ while the Mainz–Austin–Budapest version⁴⁷ of ACES II was used for CCSDT. Harmonic vibrational frequencies were predicted for the $\tilde{X}^2\Pi$ and $\tilde{A}^2\Pi$ states of OCS^+ via finite differences of energies evaluated at displaced geometries.

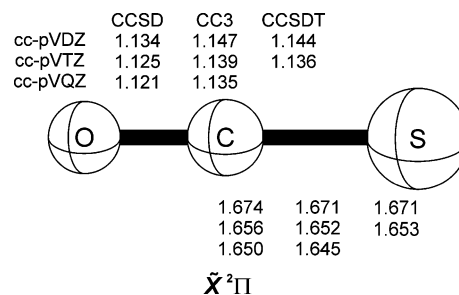


Figure 1. Optimized bond lengths (in angstroms) for the $\tilde{X}^2\Pi$ state of OCS^+ , computed at the frozen-core cc-pVXZ ($X = \text{D, T, Q}$) CCSD, CC3, and CCSDT levels of theory.

A complete quartic force field for the two Renner–Teller components of the $\tilde{A}^2\Pi$ state of OCS^+ was computed at the frozen-core cc-pVQZ EOM-CC3 level of theory and employed in concert with second-order vibrational perturbation theory (VPT2)^{48–50} to compute vibrational anharmonicity constants. The internal coordinate set employed comprised the O–C and C–S stretches and a linear O–C–S bending coordinate. The full quartic force field was computed from energies at 34 geometries displaced from the optimized frozen-core cc-pVQZ EOM-CC3 geometry (see Figure 2). The program INTDIF2005⁵¹ was used to determine the necessary displaced geometries as well as to compute the force constants in internal coordinates. The transformation of the force constants from internal to normal coordinates was performed by using INTDER2005^{52–55} while spectroscopic constants were computed with ANHARM.⁵⁵

When displaced along the O–C–S bending coordinate, the $\tilde{X}^2\Pi$ and $\tilde{A}^2\Pi$ states are split into A' and A'' components by the Renner–Teller effect.⁵⁶ Since both the A' and A'' components exhibit positive curvature with respect to the bending coordinate, and both have unique harmonic frequencies, this is a type A Renner–Teller molecule.⁵⁷ For energies at geometries displaced along this coordinate for $\tilde{A}^2\Pi$ OCS^+ , the A' state was computed via excitation from the A' component of the $\tilde{X}^2\Pi$ state while the A'' component of the $\tilde{A}^2\Pi$ state was computed relative to the A'' component of the $\tilde{X}^2\Pi$ state.

III. Results and Discussion

A. Geometries. The geometry of $\tilde{X}^2\Pi$ OCS^+ is shown in Figure 1, optimized by using CCSD, CC3, and CCSDT paired with the cc-pVXZ ($X = \text{D, T, Q}$ for CCSD and CC3; $X = \text{D, T}$ for CCSDT) basis sets. For both bond lengths, the CC3 method yields excellent agreement with results from the full CCSDT approach, offering substantial improvement over the CCSD results. The CC3 predicted C–S bond lengths are within 0.001 Å of the CCSDT results with both the cc-pVDZ and cc-pVTZ basis sets. For the C–O bond length the CC3 method overestimates the effects of triple excitations slightly, yielding C–O distances 0.003 Å larger than the CCSDT values with both the cc-pVDZ and cc-pVTZ basis sets. The corresponding absolute energies are listed in Table 1, for reference.

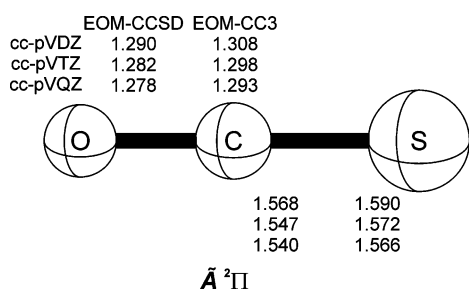
The geometry of $\tilde{A}^2\Pi$ OCS^+ was optimized by using EOM-CCSD and EOM-CC3 paired with the cc-pVXZ ($X = \text{D, T, Q}$) basis sets, as shown in Figure 2. The difference between the EOM-CCSD and EOM-CC3 optimized bond lengths is on par with those observed for $\tilde{X}^2\Pi$ OCS^+ . As such, EOM-CCSDT optimized bond lengths (which in turn should offer an excellent approximation to the full CI values) for $\tilde{A}^2\Pi$ OCS^+ would be expected to fall within 0.003 Å of those predicted by using EOM-CC3. Overall, the cc-pVQZ EOM-CC3 predicted geometry should be accurate to well within 0.01 Å. Given the sensitivity of the geometry of $\tilde{A}^2\Pi$ OCS^+ with respect to basis

TABLE 1: Absolute Energies (E , hartrees) and Harmonic Vibrational Frequencies (cm^{-1}) for the $\tilde{X}^2\Pi$ State of OCS^+ at the Corresponding Optimized Geometries (see Figure 1)

	E	ω_1	$\omega_{2,A'}$	$\omega_{2,A''}$	ω_3
cc-pVDZ CCSD	-510.341 992	682	390	442	2198
cc-pVTZ CCSD	-510.486 673	693	410	465	2219
cc-pVQZ CCSD	-510.530 820	700	413	469	2233
cc-pVDZ CC3	-510.362 393	687	376	429	2064
cc-pVTZ CC3	-510.517 127	699	394	450	2076
cc-pVQZ CC3	-510.564 159	707	396	453	2085
cc-pVDZ CCSDT	-510.360 989	685	378	431	2103
cc-pVTZ CCSDT	-510.515 012	698	397	453	2120
recommended value ^a		707	396 ^b	453 ^b	2130

^a Recommended values for ω_1 and ω_2 are from explicit cc-pVQZ CC3 computed frequencies. The value for ω_3 assumes that the cc-pVQZ CC3 prediction overestimates the effect of triple excitations by 30%.

^b Renner parameter $\epsilon = (\omega_{2,A'}^2 - \omega_{2,A''}^2)/(\omega_{2,A'}^2 + \omega_{2,A''}^2) = -0.1337$.

**Figure 2.** Optimized bond lengths (in angstroms) for the $\tilde{A}^2\Pi$ state of OCS^+ , computed at the frozen-core cc-pVXZ ($X = \text{D, T, Q}$) EOM-CCSD and EOM-CC3 levels of theory.

set and correlation method, it is not surprising that the cc-pVQZ EOM-CC3 optimized bond lengths (1.293 and 1.566 Å for R_{OC} and R_{CS} , respectively) differ by more than 0.01 Å from the ic-MRCI distances (1.279 and 1.573 Å) presented by Chen et al.²² The corresponding absolute energies are listed in Table 2.

B. Harmonic Vibrational Frequencies. Predicted harmonic vibrational frequencies for $\tilde{X}^2\Pi$ OCS^+ are provided in Table 1, computed by using CCSD, CC3, and CCSDT with the cc-pVXZ ($X = \text{D, T, Q}$) for CCSD and CC3; $X = \text{D, T}$ for CCSDT). For ω_1 and the two Renner–Teller components of ω_2 , there is excellent agreement between the CC3 and CCSDT predicted frequencies. For these two modes the CC3 approach yields predicted frequencies within 3 cm^{-1} of the CCSDT results with both the cc-pVDZ and cc-pVTZ basis sets. For the C–O stretch, however, the CC3 predicted harmonic frequency is further from the CCSDT value. For ω_3 , CC3 appears to overestimate the effect of triple excitations (i.e., the difference between the CCSD and CCSDT predicted frequencies with a given basis set) by roughly 30%: with both the cc-pVDZ and cc-pVTZ basis sets the CC3-predicted C–O stretching frequency is about 40 cm^{-1} lower than the corresponding CCSDT value. This apparent deficiency in CC3 for the C–O stretching frequency parallels the differences observed between CC3 and CCSDT optimized C–O bond lengths, mentioned above. Assuming that this 30% overestimation will similarly apply to the cc-pVQZ CC3 results, an estimated cc-pVQZ CCSDT value of 2130 cm^{-1} can be derived. This value is in good agreement with the MRCI result (2124 cm^{-1}) of Stimson et al.²¹ The available experimental values^{8,9,19} for the C–O stretching frequency are all fundamentals (and span 75 cm^{-1}), so provide no means of direct comparison with the predicted harmonic frequencies.

The two components of the Renner–Teller harmonic bending frequencies for $\tilde{X}^2\Pi$ OCS^+ are predicted to be 396 and 453 cm^{-1} at the cc-pVQC CC3 level of theory. While the A'

component (396 cm^{-1}) is in perfect agreement with the MRCI results of Stimson et al.,²¹ the harmonic frequency for the upper Renner–Teller bending frequency (453 cm^{-1}) is significantly smaller than the MRCI datum of 498 cm^{-1} . On the basis of the above comparisons of CC3 and CCSDT results with the smaller cc-pVDZ and cc-pVTZ basis sets, the presently predicted cc-pVQZ CC3 bending frequencies should be well within 5 cm^{-1} of cc-pVQZ CCSDT values, which in turn should be well-converged toward the full CI limit. The MRCI value for the A'' component appears to be too large by at least 40 cm^{-1} .

Harmonic vibrational frequencies for the $\tilde{A}^2\Pi$ state of OCS^+ are listed in Table 2, computed by using the EOM-CCSD and EOM-CC3 methods paired with the cc-pVXZ ($X = \text{D, T, Q}$) basis sets. The results exhibit a consistent convergence toward the complete basis set limit, with the cc-pVQZ results differing by less than 10 cm^{-1} from the corresponding cc-pVTZ results. In contrast to $\tilde{X}^2\Pi$ OCS^+ , both the C–S and C–O stretching frequencies are sensitive to the inclusion of triple excitations. The EOM-CC3 results are consistently 70 cm^{-1} lower than the EOM-CCSD values with a given basis set for ω_1 , while for ω_3 the EOM-CC3 results are all much smaller than the corresponding EOM-CCSD values, though the differences are far less regular. Assuming that EOM-CC3 will overestimate the effect of triple excitations in the C–O stretch by roughly 30% (as was the case for CC3 in the case of $\tilde{X}^2\Pi$ OCS^+), cc-pVQZ EOM-CCSDT would be expected to yield a value of roughly 2003 cm^{-1} .

The bending frequencies, on the other hand, are significantly less sensitive to the inclusion of triple excitations. For $\omega_{2,A'}$, the results computed with EOM-CC3 are consistently just 10 cm^{-1} smaller than the corresponding EOM-CCSD results. In the case of the upper component, partial inclusion of triple excitations via EOM-CC3 results in a slightly more significant shift in the predicted bending frequency of around 30 cm^{-1} with all three basis sets considered. This difference is of comparable size to that observed between CCSD and CC3 predictions for the bending frequencies of $\tilde{X}^2\Pi$ OCS^+ , so the final cc-pVQZ EOM-CC3 bending frequencies for the $\tilde{A}^2\Pi$ state should be similarly accurate. Regardless, the present results are certainly of sufficient quality to shed light on the disparity between the results of Somavilla and Merkt²³ and Chen et al.²²

One sees reasonable agreement between the present results and the C–S stretching frequency of Somavilla and Merkt, with the presently predicted value for ω_1 falling 10 cm^{-1} outside of the experimental range. The cc-pVQZ EOM-CC3 predicted C–O stretching frequency, however, is some 80 cm^{-1} below the experimental value (2062 \pm 6 cm^{-1}). Even “correcting” this predicted C–O stretching frequency, the final recommended value of 2003 cm^{-1} is significantly smaller than (and well outside the error bars) the result of Somavilla and Merkt.²³ The cc-pVQZ EOM-CC3 predicted average bending frequency (383 cm^{-1}) is notably smaller than that due to Chen et al.²² (417 cm^{-1}). However, this difference is almost entirely due to a difference in the predicted frequency for the upper (A') component of the Renner–Teller pair: while the two values for the A' component are within 6 cm^{-1} , the values for the A'' component differ by nearly 60 cm^{-1} . This is similar to the difference observed for the upper component of the harmonic bending frequency of $\tilde{X}^2\Pi$ OCS^+ , and may be suggestive of an unbalanced treatment of the A'' surfaces in the works of Chen et al.²² and Stimson et al.²¹ On the basis of the comparison of the presently predicted EOM-CCSD and EOM-CC3 results, the cc-pVQZ EOM-CC3 value of 401 cm^{-1} is expected to be accurate to within 10 cm^{-1} .

TABLE 2: Absolute Energies (E , hartrees) and Harmonic Vibrational Frequencies (cm^{-1}) for the $\tilde{A} \ ^2\Pi$ State of OCS^+ , at the Corresponding Optimized Geometries (see Figure 2)

	E	ω_1	$\omega_{2,A'}$	$\omega_{2,A''}$	ω_3
cc-pVDZ EOM-CCSD	-510.184 642	845	347	408	2070
cc-pVTZ EOM-CCSD	-510.327 596	856	367	428	2066
cc-pVQZ EOM-CCSD	-510.370 964	863	375	433	2059
cc-pVDZ EOM-CC3	-510.219 961	777	342	381	1943
cc-pVTZ EOM-CC3	-510.374 067	788	357	396	1970
cc-pVQZ EOM-CC3	-510.420 391	794	364	401	1979
recommended value ^a		794	364 ^b	401 ^b	2003
experiment ^c		809 \pm 6	357 \pm 5		2062 \pm 5

^a Recommended values for ω_1 and ω_2 are from explicit cc-pVQZ CC3 computed frequencies. The value for ω_3 assumes that the cc-pVQZ EOM-CC3 prediction overestimates the effect of triple excitations by 30%. ^b Renner parameter $\epsilon = -0.0965$. ^c Reference 23.

TABLE 3: Harmonic Vibrational Frequencies (ω_i), Fundamental Frequencies (ν_i), Anharmonicity Constants (x_{ij}), and Force Constants ($\Phi_{i,j,\dots}$, in Dimensionless Normal Coordinates) for the $\tilde{A} \ ^2\Pi$ State of OCS^+ , Computed at the cc-pVQZ EOM-CC3 Level of Theory (All Values Given in cm^{-1})^a

ω_1	794	Φ_{111}	162.4
ω_2	364 (401) ^b	Φ_{333}	-86.2
ω_3	1979 ^c	Φ_{122}	-116.1 (-96.5)
		Φ_{223}	-129.1 (-91.8)
ν_1	782	Φ_{113}	20.4
ν_2	359 (394)	Φ_{133}	320.2
ν_3	1966 ^d	Φ_{2222}	89.7 (50.3)
		Φ_{1111}	25.2
x_{11}	-2.0	Φ_{3333}	261.5
x_{12}	-3.5 (-2.6)	Φ_{1122}	-34.5 (-28.3)
x_{13}	-13.7	Φ_{1113}	2.9
x_{22}	1.5 (0.6)	Φ_{1223}	-26.4 (-21.7)
x_{23}	-13.0 (-12.8)	Φ_{2233}	-96.8 (-88.3)
x_{33}	0.2	Φ_{1133}	36.5
		Φ_{1133}	54.5

^a Values for the upper (A'') Renner–Teller component of the bending mode are given in parentheses. ^b Root-mean-square of the A' and A'' components = 383 cm^{-1} . ^c Recommended value 2003 cm^{-1} . ^d Recommended value 1990 cm^{-1} .

While the root-mean-squared computed harmonic bending frequency (383 cm^{-1}) is 26 cm^{-1} higher than the value of 357 \pm 5 cm^{-1} suggested by Sommovilla and Merkt,²³ it is smaller than the value proposed by Chen et al.²² (417 cm^{-1}) based on ic-MRCI computations. Perhaps more importantly, the presently predicted value for ω_2 is less than half of the predicted harmonic C–S stretching frequency (794 cm^{-1}), such that the dominant interaction between these two modes will arise from Fermi interactions between the highest components of the bending polyads with the stretching levels (as in the analysis of Sommovilla and Merkt),²³ in contrast to the assignments in the work of Chen et al.²²

C. Anharmonicity Constants. With the aim of providing a more complete description of the vibrational energy surface of the $\tilde{A} \ ^2\Pi$ state of OCS^+ , anharmonicity constants derived from the computed frozen-core cc-pVQZ EOM-CC3 quartic force field for the $\tilde{A} \ ^2\Pi$ state of OCS^+ are presented in Table 3. The theoretically predicted anharmonicity constants are generally in agreement with the available anharmonicity constants derived from the PFI-ZEKE spectrum of Sommovilla and Merkt.²³ All computed values fall within the (admittedly large) experimental error bars, with the exception of the χ_{33} value, for which the computed value (0.2 cm^{-1}) is substantially smaller than and outside of the experimental range of $-12 \pm 3 \text{ cm}^{-1}$.

IV. Summary

The Renner–Teller bending frequencies of the $\tilde{A} \ ^2\Pi$ state of OCS^+ have been examined by using the EOM-CCSD and EOM-

CC3 methods paired with the cc-pVXZ ($X = \text{D, T, Q}$) basis sets, in order to shed light on the inconsistencies between the previously reported ab initio values of Chen et al.²² and the spectroscopic determinations of Sommovilla and Merkt.²³ The seemingly subtle difference between the harmonic bending frequencies utilized by Chen et al. and Sommovilla and Merkt results in drastically different assignments of the complex and congested PFI-ZEKE spectrum. The root-mean-square of the presently predicted Renner–Teller split harmonic bending frequencies (383 cm^{-1}) is somewhat larger than the value proposed by Sommovilla and Merkt²³ (357 \pm 5 cm^{-1}) though smaller than the ic-MRCI computed values of Chen et al.²² (417 cm^{-1}). Examination of the convergence of the computed frequencies with respect to convergence of the one- and n -particle bases suggests that the presently predicted Renner–Teller bending frequencies should be accurate to within 10 cm^{-1} . The key issue in the spectral assignments is the size of this bending frequency relative to the C–S harmonic stretching frequency (predicted here to be 794 cm^{-1} ; experimental value 809 \pm 6 cm^{-1});²³ our recommended OCS bending frequency is less than half of the C–S stretching frequency, in accord with the work of Sommovilla and Merkt.²³ Thus the cc-pVQZ EOM-CC3 computed vibrational frequencies support the assignments of the PFI-ZEKE spectrum of Sommovilla and Merkt, which were markedly different than the corresponding assignments in the work of Chen et al.²² Anharmonicity constants for the $\tilde{A} \ ^2\Pi$ state of OCS^+ have also been computed, based on a cc-pVQZ EOM-CC3 quartic force field.

Harmonic vibrational frequencies were also computed for $\tilde{X} \ ^2\Pi \text{OCS}^+$ by using CCSD, CC3, and CCSDT paired with cc-pVXZ basis sets. The results demonstrate that for this system the approximate triples afforded by the CC3 method yield frequencies in excellent agreement with CCSDT for the C–S stretch and O–C–S bend, providing significant improvement over CCSD results. For the C–O stretch, on the other hand, the CC3 approach seems to overestimate the effect of connected triple excitations by roughly 30% with the cc-pVDZ and cc-pVTZ basis sets.

Acknowledgment. This work was supported by National Science Foundation, Grant No. CHE-0451445. S.E.W. would also like to thank Yukio Yamaguchi for assistance. Figures 1 and 2 were generated with HFSmol.⁵⁸

References and Notes

- (1) Tanaka, Y.; Jursa, A. S.; Leblanc, F. J. *J. Chem. Phys.* **1960**, *32*, 1205.
- (2) Horani, M.; Leach, S.; Rostas, J. *J. Chim. Phys. (Paris)* **1966**, *63*, 1015.
- (3) Turner, D. W.; May, D. P. *J. Chem. Phys.* **1967**, *46*, 1156.
- (4) Brundle, C. R.; Turner, D. W. *Int. J. Mass Spectrom. Ion Phys.* **1969**, *2*, 185.

- (5) Judge, D. L.; Ogawa, M. *J. Chem. Phys.* **1969**, *51*, 2935.
- (6) Natalis, P.; Delwiche, J.; Collin, J. E. *Faraday Discuss.* **1972**, *54*, 98.
- (7) Judge, D. L.; Lee, L. C. *Int. J. Mass. Spectrom. Ion Phys.* **1975**, *17*, 329.
- (8) Frey, R.; Gotchev, B.; Peatman, W. B.; Pollak, H.; Schlag, E. W. *Int. J. Mass Spectrom. Ion Phys.* **1978**, *26*, 137.
- (9) Delwiche, J.; Hubin-Franskin, M.-J.; Caprace, G.; Natalis, P.; Roy, D. *J. Electron Spectrosc. Relat. Phenom.* **1980**, *47*, 167.
- (10) Potts, A. W.; Fattahallah, G. H. *J. Phys. B* **1980**, *13*, 2545.
- (11) Maier, J. P.; Thommen, F. *Chem. Phys.* **1980**, *51*, 319.
- (12) Delwiche, J.; Hubin-Franskin, M.-J.; Guyon, P.-M.; Nenner, I. *J. Chem. Phys.* **1981**, *74*, 4219.
- (13) Ono, Y.; Osuch, E. A.; Ng, C. Y. *J. Chem. Phys.* **1981**, *74*, 1645.
- (14) Kovač, B. *J. Chem. Phys.* **1983**, *78*, 1684.
- (15) Ochsner, M.; Tsuji, M.; Maier, J. P. *Chem. Phys. Lett.* **1985**, *115*, 373.
- (16) Kakoschke, R.; Boesl, Y.; Herman, J.; Schlag, E. W. *Chem. Phys. Lett.* **1985**, *119*, 467.
- (17) Wu, C. Y. R.; Yih, T. S.; Judge, D. L. *Int. J. Mass Spectrom. Ion Phys.* **1986**, *68*, 303.
- (18) Tsuji, M.; Maier, J. P. *Chem. Phys. Lett.* **1987**, *137*, 421.
- (19) Wang, L.-S.; Reutt, J. E.; Lee, Y. T.; Shirley, D. A. *J. Electron Spectrosc. Relat. Phenom.* **1988**, *47*, 167.
- (20) Hubin-Franskin, M.-J.; Delwiche, J.; Guyon, P.-M.; Richard-Viard, M.; Lavollée, M.; Dutuit, O.; Robbe, J.-M.; Flament, J.-P. *Chem. Phys.* **1996**, *209*, 143.
- (21) Stimson, S.; Evans, M.; Ng, C. Y.; Hsu, C.-W.; Heimann, P.; Destandau, C.; Chambaud, G.; Rosmus, P. *J. Chem. Phys.* **1998**, *108*, 6205.
- (22) Chen, W.; Hochlaf, M.; Rosmus, P.; He, G. Z.; Ng, C. Y. *J. Chem. Phys.* **2002**, *116*, 5612.
- (23) Somavilla, M.; Merkt, F. *J. Phys. Chem. A* **2004**, *108*, 9970.
- (24) Takeshita, K.; Shida, N.; Miyoshi, E. *Theor. Chem. Acc.* **1998**, *107*, 33.
- (25) Chen, B.-Z.; Huang, M.-B.; Chang, H.-B. *Chem. Phys. Lett.* **2005**, *416*, 107.
- (26) Chen, B.-Z.; Chang, H.-B.; Huang, H. C. *J. Chem. Phys.* **2006**, *125*, 054310.
- (27) Hirst, D. M. *Mol. Phys.* **2006**, *104*, 55.
- (28) Masuda, S.; Hatsui, T.; Kosugi, N. *J. Electron Spectrosc. Relat. Phenom.* **2004**, *137–140*, 351.
- (29) Yamaguchi, Y.; Schaefer, H. F. *J. Chem. Phys.* **2004**, *120*, 9536.
- (30) Purvis, G. D.; Bartlett, R. J. *J. Chem. Phys.* **1982**, *76*, 1910.
- (31) Scuseria, G. E.; Janssen, C. L.; Schaefer, H. F. *J. Chem. Phys.* **1988**, *89*, 7382.
- (32) Scuseria, G. E.; Scheiner, A. C.; Lee, T. J.; Rice, J. E.; Schaefer, H. F. *J. Chem. Phys.* **1987**, *86*, 2881.
- (33) Rittby, M.; Bartlett, R. J. *J. Phys. Chem.* **1988**, *92*, 3033.
- (34) Christiansen, O.; Koch, H.; Jørgensen, P. *J. Chem. Phys.* **1995**, *103*, 7429.
- (35) Koch, H.; Christiansen, O.; Jørgensen, P.; de Merás, A. M. S.; Helgaker, T. *J. Chem. Phys.* **1997**, *106*, 1808.
- (36) Koch, H.; Christiansen, O.; Jørgensen, P.; Olsen, J. *Chem. Phys. Lett.* **1995**, *244*, 75.
- (37) Noga, J.; Bartlett, R. J. *J. Chem. Phys.* **1987**, *86*, 7041.
- (38) Noga, J.; Bartlett, R. J. *J. Chem. Phys.* **1988**, *89*, 3401.
- (39) Watts, J. D.; Bartlett, R. J. *J. Chem. Phys.* **1990**, *93*, 6104.
- (40) Scuseria, G. E.; Schaefer, H. F. *Chem. Phys. Lett.* **1988**, *152*, 382.
- (41) Dunning, T. H. *J. Chem. Phys.* **1989**, *90*, 1007.
- (42) Stanton, J. F.; Bartlett, R. J. *J. Chem. Phys.* **1993**, *98*, 7029.
- (43) Stanton, J. F.; Gauss, J. *Theor. Chim. Acta* **1995**, *91*, 267.
- (44) Smith, C. E.; King, R. A.; Crawford, T. D. *J. Chem. Phys.* **2005**, *122*, 054110.
- (45) Sattelmeyer, K. W.; Stanton, J. F.; Olsen, J.; Gauss, J. *Chem. Phys. Lett.* **2001**, *347*, 499.
- (46) Crawford, T. D.; Sherrill, C. D.; Valeev, E. F.; Fermann, J. T.; King, R. A.; Leininger, M. L.; Brown, S. T.; Janssen, C. L.; Seidl, E. T.; Kenny, J. P.; Allen, W. D. *Psi 3.2*, 2003.
- (47) Stanton, J. F.; Gauss, J.; Watts, J. D.; Szalay, J. G.; Bartlett, R. J.; with contributions from Auer, A. A.; Bernholdt, D. B.; Christiansen, O.; Harding, M. E.; Heckert, M.; Heun, O.; Huber, C.; Jonsson, D.; Jusélius, J.; Lauderdale, W. J.; Metzroth, T.; Michauk, C.; Price, D. R.; Ruud, K.; Schiffmann, F.; Tajti, A.; Varner, M. E.; Vázquez, J. and the integral packages: MOLECULE (J. Almlöf and P. R. Taylor), PROPS (P. R. Taylor), and ABACUS (T. Helgaker, H. J. Aa. Jensen, P. Jørgensen, and J. Olsen). See, also Stanton, J. F.; Gauss, J.; Watts, J. D.; Lauderdale, W. J.; Bartlett, R. J. *Int. J. Quantum Chem. Symp.* **1992**, *26*, 879. Current version see <http://www.aces2.de>.
- (48) Nielsen, H. H. *Rev. Mod. Phys.* **1951**, *23*, 90.
- (49) Watson, J. K. G. VPT2. In *Vibrational Spectra and Structure*; Durig, J. R., Ed.; Elsevier: Amsterdam, The Netherlands, 1977; p 1.
- (50) Papoušek, D.; Aliev, M. R. *Molecular Vibrational-Rotational Spectra*; Elsevier: Amsterdam, The Netherlands, 1982.
- (51) INTDIF2005 is an abstract program written by Wesley D. Allen for *Mathematica* (Wolfram Research, Inc., Champagne, Illinois) to perform general numerical differentiation to high orders of electronic structure data.
- (52) INTDER2005 is a general program written by W. D. Allen that performs sundry vibrational analyses and higher order nonlinear transformations among force field representations.
- (53) Allen, W. D.; Császár, A. G.; Szalay, P. G.; Mills, I. M. *Mol. Phys.* **1996**, *89*, 1213.
- (54) Allen, W. D.; Császár, A. G. *J. Chem. Phys.* **1993**, *98*, 2983.
- (55) See program descriptions in: Sarka, K.; Demaison, J. In *Computational Molecular Spectroscopy*; Jensen, P., Bunker, P. R., Eds.; Wiley: Chichester, UK, 2000; p 255.
- (56) Renner, R. Z. *Phys.* **1934**, *92*, 172.
- (57) Lee, T. J.; Fox, D. J.; Schaefer, H. F.; Pitzer, R. M. *J. Chem. Phys.* **1984**, *81*, 356.
- (58) Wheeler, S. E. HFSmol, 2005.